Fabrication of Catheter-tip and Sidewall Miniature Pressure Sensors

Fabrication of Catheter-Tip and Sidewall Miniature Pressure Sensors

MASAYOSHI ESASHI, HIROSHI KOMATSU, TADAYUKI MATSUO, SENIOR MEMBER, IEEE, MASAFUMI TAKAHASHI, TAMOTSU TAKISHIMA, KENICHI IMABAYASHI, AND HIDEO OZAWA

Abstract—Silicon-diaphragm miniature pressure sensors, which use the piezoresistive effect, were developed for biomedical applications. We fabricated two types of sensors; that is, a catheter-tip (1.2-mm outside diameter, 0.17 mm thick) and a sidewall (1.4 × 3.45 × 0.22 mm) sensor, both having a thin circular diaphragm. Their diaphragms, 10 μm in thickness and 0.55 mm in diameter, were formed by an electrochemical etching method.

Since the stability of pressure sensors is the most important requirement for precise pressure measurements, attractive approaches have been investigated to improve stability. The major instabilities of the present miniature pressure sensors are electrical drifts caused by leakage currents and thermal disturbances related to packaging stress. A shield and a guard plate can prevent the device from leakage currents. A thick supporting rim structure of the sensor and mounting on a stainless steel support with elastic material contribute to eliminate the packaging stress.

For the purpose of easy lead attachment to the catheter-tip sensor, we use a unique structure having deep contact holes in deposited thick polysilicon layer (0.05 mm thick).

Experimental results are as follows: Initial drift after power up was improved to about one tenth. Thermal disturbances, as temperature zero shift, thermal transient response, and temperature cycle hysteresis were greatly reduced. Low-temperature zero shift of 0.2 mmHg/°C was obtained using a simple temperature compensation method. Long-term drift was 0.6 mmHg/day.

The catheter of 1.8-mm outer diameter having two sidewall sensors has been satisfactorily used for the study of urodynamics.

I. INTRODUCTION

IN BIOMEDICAL RESEARCH, the need for small reliable pressure sensor is without question. By taking advantage of the advanced state of the art for integrated circuit processing, miniature pressure sensors of high sensitivity can be batch fabricated with high yield at low cost. Several papers concerning silicon-diaphragm pressure sensors for catheter-tip and implantable applications have appeared in recent years [1]-[6]. There are many kinds of sensors such as piezoresistive or capacitive pressure sensors, the absolute pressure sensor for implantation, or active sensors which contain monolithic signal-conditioning circuits.

For the monitoring of low pressures, such as intraveneous pressure, urinary pressure, or esophageal pressure, sensor stability is essential. However, in present miniature pressure sensors, this sensor stability, which is a common and fundamental problem for any type of pressure sensor, has not been satisfactorily resolved and restricts the use of these devices [3].

The main purpose of this paper is to find possible solutions to piezoresistive sensor instabilities such as electrical drift or thermal disturbance. It is considered that the electrical drift is caused mainly by surface leakage and reverse-biased p-n junction leakage currents, and the thermal disturbances are caused by the mismatch of thermal expansion coefficients between the sensor chip and its supporting material. The main feature of our approach to improve sensor stability is to obtain a low electrical drift by the use of suitable shielding and guard structure to reduce the leakage current, and to eliminate the thermal disturbances by use of a thick supporting rim structure and elastic bonding material for its mounting.

At the same time, to satisfy various medical requirements, we have fabricated two types of pressure sensor; one is a sidewall mounted sensor, the other is a catheter-tip sensor. They have the same circular diaphragm fabricated by electrochemical etching technique.

It is easy to assemble a multichannel-sensor catheter, which is advantageous to measure local pressures at several points simultaneously [4]. We have developed a two-channel-sensor catheter and applied it for the study of urodynamics.

II. DESIGN CONSIDERATIONS

A. Piezoresistive Effect

Silicon-diaphragm pressure sensors are very common as miniature pressure sensors and their advantages are described in many other papers [1]-[6]. Sensing elements of diffused piezoresistors are fabricated at the surface of a thin circular or square diaphragm. The stress magnification properties of a clamped circular diaphragm are proportional to the square of the ratio of the diaphragm radius to its thickness. For a diaphragm diameter of 0.5 mm, a 0.01-mm thickness is required to obtain a reasonable sensitivity.

The stress pattern on a circular diaphragm is simple and the design principle of the piezoresistors' arrangement has been established [1]. For p-type resistors oriented in the [110] direction on a (100) diaphragm plane, the fractional changes in the piezoresistors due to the pressure-induced stress are given as follows [1]:

$$\left(\frac{\Delta R}{R}\right)_r = -\left(\frac{\Delta R}{R}\right)_t = -\pi_{44}\frac{3Pa^2}{8h^2}(1-\nu) \quad (1)$$

Manuscript received May 18, 1981; revised September 14, 1981. This work was supported in part by the Japanese Ministry of Education, Science and Culture under Grants-in-Aid for Scientific Research No. 485105, 1979, and No. 575254, 1980.

M. Esashi, H. Komatsu, and T. Matsuo are with the Department of Electronic Engineering, Tohoku University, Sendai, Japan.

M. Takahashi, T. Takishima, and K. Imabayashi are with the School of Medicine, Tohoku University, Sendai, Japan.

H. Ozawa is with Nihon Kohden Ltd., Tokyo, Japan.

0018-9383/82/0100-0057$00.75

where

r and t	radial and tangential resistors, respectively,
π_{44}	dominant piezoresistive coefficient in p-type piezoresistor,
P	pressure,
h	diaphragm thickness,
ν	Poisson's ratio,
a	distance from the center.

The above equation shows that the fractional changes in radial and tangential resistors have the opposite sign but the same magnitude of piezoresistivity. Therefore, by connecting these sensing resistors in series, we can get high-pressure sensitivity of $\pi_{44}(3a^2/16h^2)\ (1-\nu)$ for half-bridge and $\pi_{44}(3a^2/8h^2)\,(1-\nu)$ for full-bridge configurations.

The value of the sheet resistivity of the piezoresistors was determined as follows: By going to high doping, we cannot get proper pressure sensitivity; however, light doping should be avoided to prevent the influence of parasitic leakage resistance. In this study, we adopted a sheet resistivity of 200 Ω/□ and 2 kΩ for each sensing resistor. A half-bridge configuration is used for a sidewall sensor and a full bridge is used for a catheter-tip sensor.

B. Electrical Drift

There are several types of leakage currents in the piezoresistive pressure sensor. They shunt the sensing resistors and their fluctuations cause initial and long-term drifts of the sensor output. To improve the electrical drift, we considered the following two dominant leakage currents among them; that is, one, a surface leakage current on the SiO_2 passivation film and the other, the leakage current across the field-induced p-n junction of the diffused resistors. The latter is modulated by the fluctuation of the electric field on the surface, that is, a gate-controlled-diode operation. It is supposed that surface impurities such as ions or moisture are responsible for such currents and they are polarized gradually by the applied voltage to the bridge.

As an example, a fluctuation of a surface leakage resistance of 300 MΩ (assumed) is equivalent to a pressure change of 1 mmHg under the condition of 3-kΩ piezoresistors and a 10-ppm/mmHg pressure sensitivity. Such a leakage resistance must be avoided.

The leakage current on SiO_2 surface can be reduced by a metal guard ring surrounding the signal terminal. By using the guard-ring structure, the elastic field between the guard ring and the signal terminals (refer to Fig. 1) disappears and the surface leakage current does not flow into the signal terminal, hence the drift due to this current can be eliminated. On the other hand, the problem of the leakage current across the field-induced p-n junction can be solved by a shield metallization applied on the chip surface.

These above two stabilization methods are realized simultaneously by the circuit configuration given in Fig. 1. In this configuration, a half bridge is used and a shield plate is deposited over the sensing resistors and it also serves as a guard layer surrounding the signal terminal. This shield plate is effective to keep the SiO_2 surface potential constant, and therefore, it can eliminate the leakage current across the field-induced p-n junction. This shield plate is connected to the output of a voltage follower which detects the sensor output and hence there is no potential difference between the signal terminal and the shield plate. This plate, therefore, serves as the guard layer and no leakage current will flow into the signal terminal.

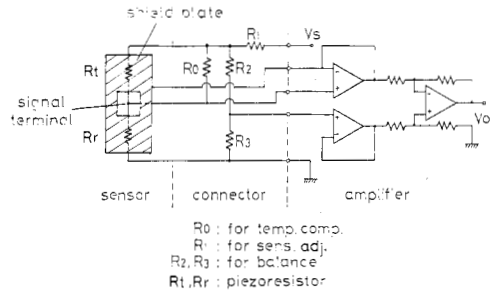

Fig. 1. Bridge circuit of a sidewall sensor.

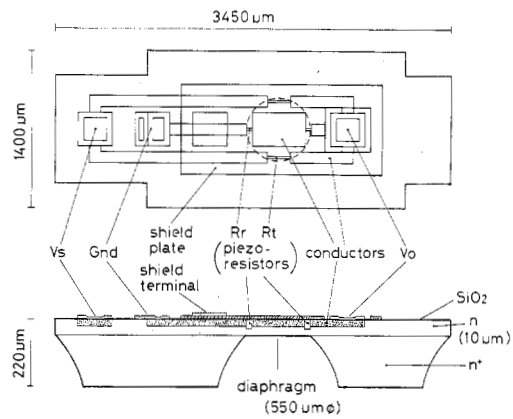

Fig. 2. Chip structure of a sidewall sensor.

Fig. 2 shows the structure of the sidewall sensor with the shield plate; here a Cr shield layer is evaporated over the surface of the piezoresistors, also surrounding the signal terminal and serving as a guard.

C. Thermal Disturbance

Thermal effects such as the temperature drift of the offset voltage, the temperature cycle hysteresis, and the transient response to an abrupt temperature change could arise in a mounted pressure sensor due to the additional stress caused by a mismatch in the thermal expansion coefficients between the sensor and its support. For this reason, the device structure should be designed considering the packaging problem.

Some excellent packaging methods have been invented. One example is a silicon chip bonded to a material with a similar temperature coefficient by electrostatic sealing [2]. Another example is that of two similarly shaped silicon chips bonded back to back with a eutectic alloy [3].

The approach in this paper is to fabricate the supporting rim of the diaphragm as thick as possible to reduce the packaging stress. The method of bonding the sensor chip to the support

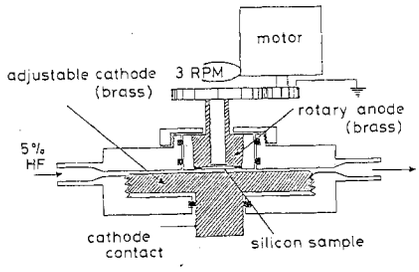

Fig. 3. Electrochemical etching apparatus of a silicon wafer.

is also integral in obtaining sensor stability. An elastic bonding material is preferable, because it can serve as a buffer for the stress due to the mismatch in the thermal expansion coefficients previously described.

III. Fabrication

To satisfy various medical requirements, we fabricated two types of pressure sensors; that is, one is a sidewall-mounted sensor and the other is a catheter-tip sensor. They have the same circular diaphragm, but different supporting rim structures; that is, their geometries are compatible with sidewall and catheter-tip mounting methods, respectively.

As these different supporting rim structures have to be fabricated by different processes, we explain these processes separately as follows.

A. Thin-Diaphragm Fabrication by Electrochemical Etching

Anisotropic etching of silicon has been generally used to fabricate thin silicon diaphragms until now, but the method is not suitable for forming a circular diaphragm.

In this work, a technique of selective electrochemical etching to form flat, circular diaphragms has been developed. The starting material is a (100)-oriented epitaxial wafer of 0.22-mm thickness, which is composed of an n^+-type substrate of 0.01 $\Omega \cdot$ cm and an epitaxially grown n-type layer of 10 μm in thickness and 10 $\Omega \cdot$ cm. Electrochemical etching has the feature that n^+-type silicon is readily etched, while n-type silicon is not [7]. The etching speed ratio is about one thousandth. For this reason, highly doped n^+-type substrate can be selectively etched away and a thin and flat n-type diaphragm which is 0.55 mm in diameter and 10 μm in thickness is obtained. The uniformity of finished diameter is about ±5 percent.

This electrochemical etching system actually used is shown in Fig. 3, where the anode and cathode are kept as close as possible (approximately 0.5 mm apart) and the 5-percent HF solution is flowing between these electrodes. Since the amount of removed material is proportional to the charge through the cell, the etching behavior can be monitored with a cell current integrator. The experimental results as shown in Fig. 4, in which, diameters D, d, and depth h are plotted at every 1×10^{-5} C. From this figure, a 550-μm diameter can be obtained at the point of 5.2×10^{-5} C (part (c) in the figure).

Since the wafer is oxidized after diaphragm formation by electrochemical etching, both sides of the completed diaphragm of the sensor are covered with an SiO_2 layer. This

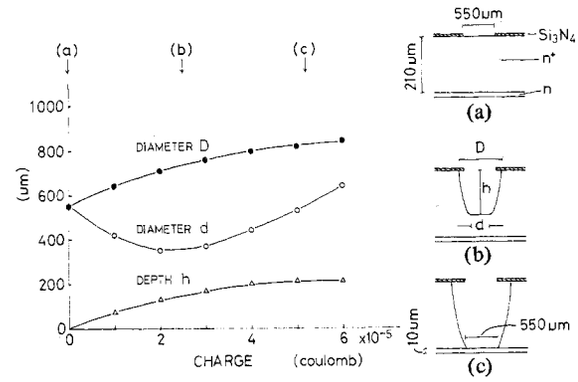

Fig. 4. Dependence of etched profile of (100) silicon wafer with charge through the etching cell. The anode voltage is 5 V, and the current is 30 to 80 mA. The cross sections of the wafer are shown; (a), (b), and (c).

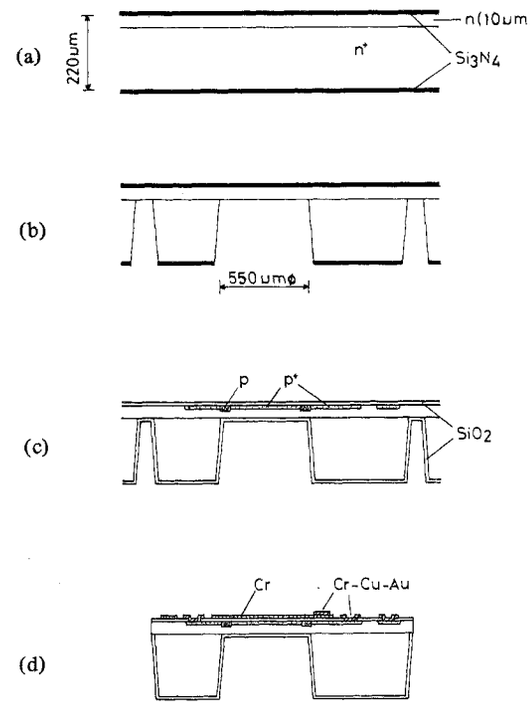

Fig. 5. Fabrication process of a sidewall sensor. (a) Silicon epitaxial wafer deposited with silicon nitride. (b) Fabrication of diaphragm by electrochemical etching. (c) Diffusion of sensing resistors and conductors. (d) Metallization and chip separation.

SiO_2-Si-SiO_2 structure can compensate the stress induced by the difference of expansion coefficients between Si and SiO_2 [1].

B. Fabrication Process for the Sidewall Sensor

Eight sensors are batch fabricated from one 12-mm square wafer. The outline of the sidewall sensor fabrication process is shown in Fig. 5, and the sequence is as follows:

1) Silicon nitride (Si_3N_4) layers (3000 Å in thickness) are deposited on both faces of the silicon epitaxial wafer as a mask for electrochemical etching [Fig. 5(a)].

2) After initial patterning of the substrate side with Si_3N_4 etching by hot phosphoric acid (170°C, 2 h), the diaphragm is

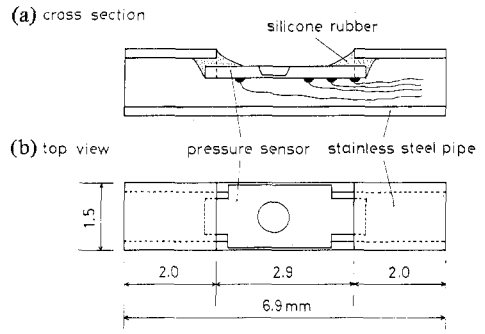

Fig. 6. Assembled sidewall sensor.

formed using electrochemical etching [Fig. 5(b)]. This etching takes about 40 min.

3) Si_3N_4 is stripped off by a 50-percent HF etchant and the wafer is oxidized. p-type sensing resistors are next defined and boron is diffused from a liquid diffusion source (BBr_3).

4) After patterning, p^+ conductors which connect sensing resistors and contact pads are diffused [Fig. 5(c)].

5) Contact holes are opened, and after Cr evaporation (about 3000 Å in thickness), the shield plate pattern is formed by photolithography.

6) Each of the sensors are separated from the wafer by Si etching ($HF:HNO_3:CH_3COOH = 12:1:2$) and scribing [Fig. 5(d)]. The lead wires, applying emulsified lead-tin solder to the tip, are brought in contact with the pads and the whole structure is heated to melt the solder. The sensor chip is mounted on a stainless steel pipe support of 1.5-mm outer diameter, which is finally packaged in a catheter (1.8-mm outer diameter).

The assembled sidewall sensor is shown in Fig. 6. The shape of the sensor chip is designed to be easily built into a stainless steel pipe support. Sensing resistors and lead wires are faced to the inside of the catheter and are prevented from direct contact with blood or fluid.

C. Fabrication Process for the Catheter-Tip Sensor

The catheter-tip sensor is designed to facilitate lead attachment. A thick polysilicon layer of 0.05 mm in thickness is deposited and deep contact holes of 0.15-mm outside diameter in this polysilicon act as the guide for lead wire soldering. A full bridge configuration with four arm resistors is used and the shield metallization is not applied to this catheter-tip sensor for simplicity.

Fig. 7 shows the outline of the catheter-tip sensor fabrication process:

1) Thin diaphragm and p-type sensing resistors are formed. The process sequence is the same as that for the sidewall sensor for process steps 1) to 3).

2) After opening the contact holes [Fig. 7(a)], the Si_3N_4 layer and the thick polysilicon layer are deposited [Fig. 7(b)]. This polysilicon was deposited from SiH_4 at relatively low temperature (700°C) to prevent the wafer from bending.

3) The wafer is oxidized and Si_3N_4 is deposited.

4) After patterning, Si_3N_4, SiO_2, and polysilicon layers are etched away successively [Fig. 7(c)]. Polysilicon is etched by a Si etchant ($HF:HNO_3:CH_3COOH = 12:1:2$).

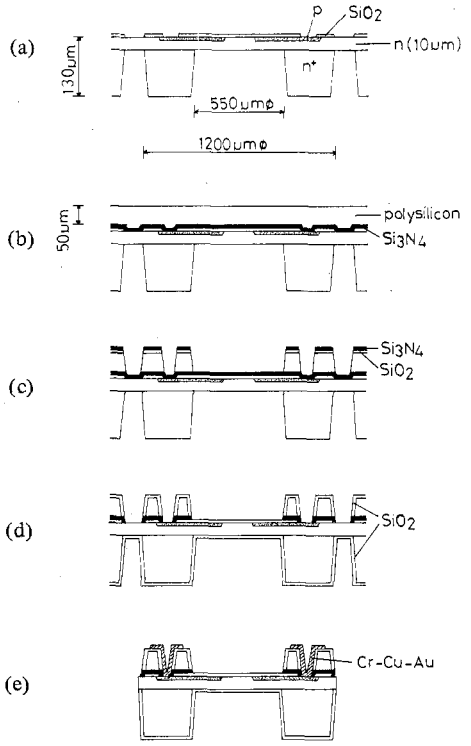

Fig. 7. Fabrication process of a catheter-tip sensor. (a) Diffusion of sensing resistors and contact hole opening. (b) Deposition of silicon nitride and thick polysilicon (about 0.05 mm). (c) Etching of polysilicon layer using silicon nitride as a mask. (d) Oxidation of polysilicon and contact hole reopening by silicon nitride etching. (e) Metallization and chip separation.

5) The wafer is next oxidized (4000 A) to insulate the polysilicon sidewall which has been exposed by etching. Contact holes are reopened by Si_3N_4 etching [Fig. 7(d)].

6) Successive layers of Cr-Cu-Au are evaporated through a metal mask about 1 μm in total thickness.

7) After separation of each sensor chip by Si etching [Fig. 7(e)], lead wires of 0.06-mm outside diameter are soldered and then the chip is mounted to a stainless steel pipe support with epoxy, which is finally assembled to a catheter tip.

The assembled catheter-tip sensor is shown in Fig. 8 and the photographs of a catheter-tip sensor are shown in Fig. 9. Like the sidewall sensor assembly in Fig. 6, the diffused resistors of this sensor are not exposed to outer fluid. The thick polysilicon layer can also serve as a guide for attachment of the sensor to the support. The increased sensor thickness is also helpful to the thermal stability of the sensor for the reason discussed in Section II-C.

Finally, the outer surface of the sensor is covered with a protective overcoat of an opaque silicone rubber. This overcoat is also effective in preventing sensor artifacts due to light, and causes no change in sensitivity or hysteresis.

IV. Experimental Results

A. Basic Characteristics

A test setup having a controlled temperature water bath (within ±0.2°C) was used to evaluate the pressure sensors. The basic characteristics described in this section are similar for both the sidewall sensor and the catheter-tip sensor. How-

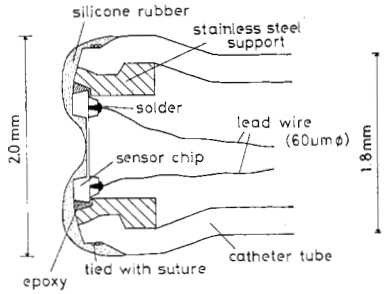

Fig. 8. Assembled catheter-tip sensor.

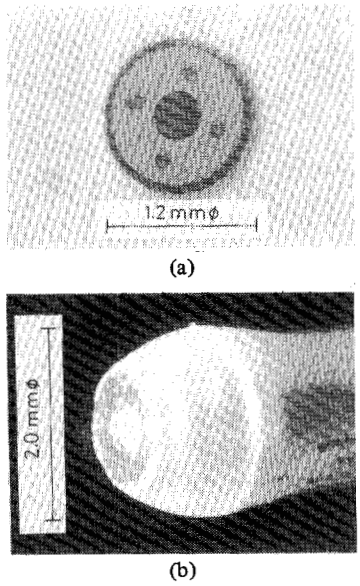

Fig. 9. Photographs of a catheter-tip sensor. (a) Chip surface. (b) Assembled to PVC tube.

ever, in the following Sections IV-B and IV-C, we will discuss the characteristics of sidewall sensors. The sensitivities of these sensors are in the range from 11 to 14 $\mu V/V_{supply}$/mmHg. No nonlinearity or hysteresis caused by pressure cycling has been observed within the limits of pressure found in the human body (0 to 300 mmHg). The temperature coefficient of sensitivity is typically -2500 ppm/°C, which corresponds to data reported earlier [4].

B. Electrical Drift

An initial drift is ordinarily observed after the device is powered up at a constant temperature (for example, 37°C). This problem has been nearly solved by the shield-plate structure. Fig. 10(a) and (b) shows typical examples of an electrical drift of the sidewall sensors which have a supporting rim of 0.22 mm in thickness and are bonded to the support with silicone rubber. Fig. 10(a) displays the data given by the device with the shield plate, and while Fig. 10(b) displays data without the shield. The shield plate improved the stability during a 4-h turn-on transient. The advantage of the shield plate in suppressing the initial drift is clear.

On the other hand, the improved sensor shows some drift in the period from 4 to 17 h after the turn on. This drift also depends on the supply voltage. For example, after the initial 10 h, the drift rate at a supply voltage of 2 V was 0.07 mmHg/h, while that at 4 V was 0.12 mmHg/h. This drift rate of 0.12 mmHg/h corresponds to the leakage current change of 1.3 nA/h. These data show that the drift can be reduced by decreasing the supply voltage, but the mechanism of this is unclear at present.

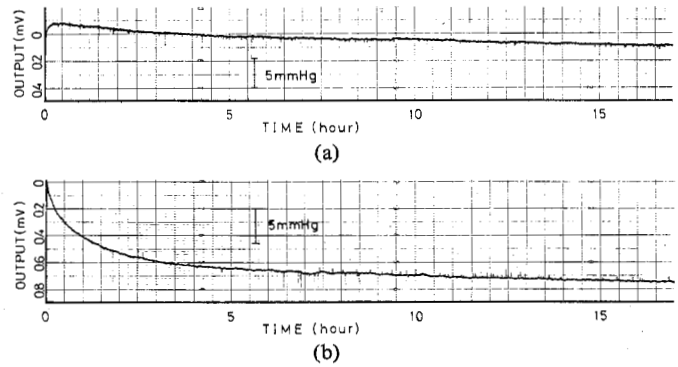

Fig. 10. Electrical drift of a sidewall sensor after power up (V_{supply} = 4 V). (a) With shield plate. (b) Without shield plate.

The long-term drift is typically 0.6 mmHg/day after three-days run.

C. Thermal Disturbance

A typical output zero shift with temperature corresponds to a pressure change of 3 mmHg/°C (average value between 20 and 37°C). As this value is similar for the device both before and after bonding with silicone rubber (Corning Co. RTV 3140), the cause of its temperature zero shift is considered to be dominated by differences in the temperature coefficients of the piezoresistors.

On the other hand, devices which were bonded eutectically to a stainless steel pipe support with Au-Sn alloy (80 percent Au-20 percent Sn) showed a large temperature zero shift of about 30 mmHg/°C. This large shift is apparently caused by the stress due to the mismatch of the thermal expansion coefficients between the sensor chip and the stainless steel pipe (the coefficient of linear expansion for Si is 2.4×10^{-6}/°C and for stainless steel 16.4×10^{-6}/°C).

The temperature zero shifts of these sensors are so large that temperature compensation by an external circuit is essential to biomedical measurements. This compensation method will be discussed later.

The transient response to an abrupt temperature change and hysteresis due to temperature cycling are important problems, since they are nearly impossible to compensate. These problems depend to a great extent on the packaging method.

Examples of 1-h response after an abrupt temperature change from 20 to 37°C are shown in Fig. 11. The difference in response between the devices with different supporting rim thickness, bonding material, and shield plate can be seen by comparing the curves of Fig. 11. These phenomena are considered to be caused by gradual plastic deformation of adhesive resin due to the temporal packaging stress originated in the temperature nonuniformity.

By comparing curves (*c*), (*d*) and (*e*), it is confirmed that the thick (0.22-mm) supporting rim structure shows a smaller tran-

	supporting rim thickness	shield plate	bonding material	drift rate after initial one hour
a	220 μm	without	epoxy	5.0 mmHg/hour
b	220	with	Au-Sn alloy	2.7
c	220	without	silicone rubber	0.9
d	220	with	silicone rubber	1.1
e	120	with	silicone rubber	5.5

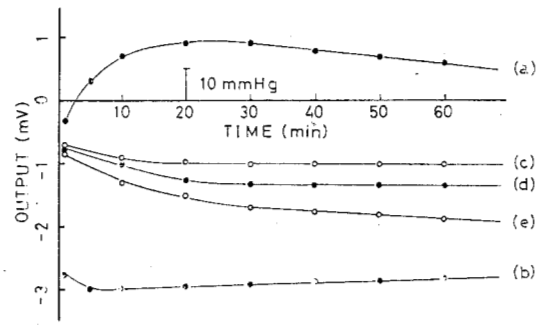

Fig. 11. Examples of transient response of sidewall sensors to an abrupt temperature change from 20 to 37°C. The table shows the experimental conditions and drift rates after initial 1 h of each response curves ((*a*)-(*e*)).

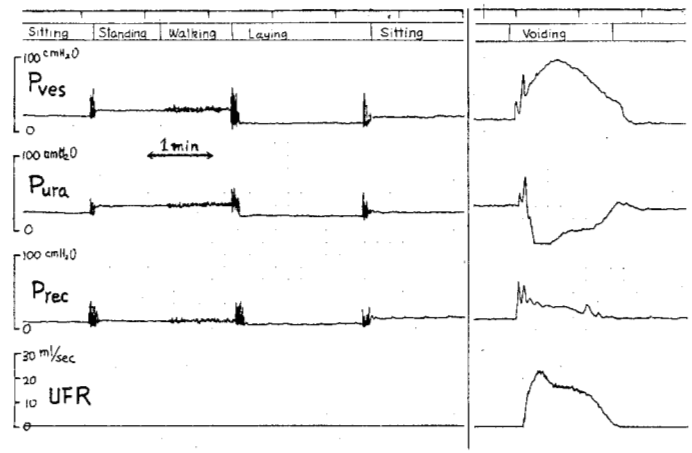

Fig. 12. A result obtained from a clinical case with normal voiding pattern. The traces, from top to bottom, revealed intravesical pressure (P_{ves}), intraurethral pressure (P_{ura}), intrarectal pressure (P_{rec}), and uroflow rate (UFR), respectively. The former two were recorded simultaneously using a two-channel-sensor catheter, and P_{rec} was recorded by another similar catheter. The effect of postural change on these parameters is shown in the left half, and a voiding pattern was shown in the right half. P_{ves} had elevated significantly at voluntary voiding, and it was followed by marked decrease of P_{ura}, resulting in micturition, which could be seen by the rise of the UFR trace.

sient response than the thin (0.12-mm) one. Besides, smaller transient responses were observed with the devices bonded with elastic silicone rubber (curves (*c*), (*d*)) rather than that with relatively stiff epoxy resin (curve (*a*)). The device eutectically bonded with the Au-Sn alloy (curve (*b*)) has a large output zero shift caused by a temperature change, but shows a relatively small transient response to an abrupt temperature change. The reason is considered that the stress applied to the diaphragm is large because of a large thermal expansion coefficient difference between the sensor chip and the support material, but the transient response of the stress is small because of its rigid structure and the small thermal time constant of the stainless steel support.

The drift rates after the initial 1 h are shown in the table of Fig. 11. The sensors (*c*) and (*d*), which are using a thick supporting rim structure and the elastic bonding material, also show the least drift rate (0.9 and 1.1 mmHg/h, respectively).

The temperature cycle hysteresis of the sidewall devices, which have thick supporting rims of 0.22-mm thickness and are bonded on stainless steel pipe supports with silicone rubber, is less than 1 mmHg/°C. On the other hand, the temperature cycle hysteresis of the devices with supporting rims of 0.12-mm thickness or those bonded on a stainless steel support with epoxy or Au-Sn alloy cannot be evaluated because of their large zero drift as shown in Fig. 11.

These experiments point out to the superiority of the packaging method using the thick supporting rim structure and the elastic bonding material.

V. Temperature Compensation and Interface Circuits

Sensitivity calibration, zero correction, and temperature compensation are necessary for each pressure sensor. These problems will be solved by making every sensor's characteristics uniform by incorporating four metal-film resistors within a connector as shown in Fig. 1. In this figure, R_0 is for temperature compensation, R_1 is for pressure sensitivity adjustment, R_2 and R_3 compose a full bridge with sensing resistors (R_t, R_r) and are used to adjust the offset voltage. Typical values for R_2, R_3 are 2 kΩ, and for R_1 is 550 Ω.

The temperature compensation method for a half-bridge-type sensor is simple and explained as follows. At first, the resistance values of each piezoresistor R_t and R_r are measured at temperatures T_1 and T_2 ($T_1 > T_2$) and they are denoted as R_{t1}, R_{r1}, R_{t2}, and R_{r2}, respectively. Under the temperature-compensating condition, the ratio of $(1/R_t + 1/R_0)^{-1}$ and R_r should coincide at both temperatures T_1 and T_2, as given below

$$\frac{R_{r1}}{(1/R_{t1} + 1/R_0)^{-1}} = \frac{R_{r2}}{(1/R_{t2} + 1/R_0)^{-1}} \tag{2}$$

and, therefore,

$$R_0 = \frac{R_{t1}R_{t2}(R_{r2} - R_{r1})}{R_{r1}R_{t2} - R_{r2}R_{t1}}. \tag{3}$$

The value of R_0 is given by (3). If R_0 is negative, it should be connected parallel to R_r. This method is simple and easy and a temperature coefficient of about 0.2 mmHg/°C can be obtained after compensation.

VI. Medical Applications

The pressure sensors described above are being applied in several medical applications. A soft and small-sized urethral catheter, 1.8-mm outer diameter PVC tube, which contains two sidewall sensors, was developed for the study of urodynamics. Fig. 12 shows a result obtained from a clinical case with normal voiding pattern. In this application, the intraves-

ical and intraurethral pressures are recorded simultaneously by this two-channel-sensor catheter.

This sensor has also been used to monitor the pressure waveform in heart ventricles in animal studies. In this case, a sidewall sensor was mounted on a teflon catheter tube.

The catheter can be soaked in disinfectant by sealing the connector part with a cap to prevent the catheter tube from the infusion of disinfectant.

VII. Conclusion

Miniature pressure sensors for biomedical application have been developed. We have placed great emphasis on improving the stability of such devices by reducing effects such as initial drift, temperature drift, temperature cycle hysteresis, and the transient response to an abrupt temperature change. Some of these instabilities, which are mainly thermal disturbances, have a common origin due to the packaging stress. They are improved by bonding a thick supporting rim sensor structure to a stainless steel support with an elastic silicone rubber. This thick sensor structure was obtained using electrochemical etching to form a thin silicon diaphragm.

The problem of initial drift during a 4-h turn-on transient was greatly reduced by a surface metallization which serves as a shield and guard plate to prevent leakage currents.

Catheter-tip and sidewall sensors for the multichannel-sensor catheter were fabricated. Two-channel-sensor catheter was applied satisfactorily for the study of urodynamics.

Further detailed research is required to develop complete and totally satisfactory, long-term stable, miniature pressure sensors.

References

[1] Samaun, K. D. Wise, and J. B. Angell, "An IC piezoresistive pressure sensor for biomedical instrumentation," *IEEE Trans. Biomed. Eng.*, vol. BME-20, pp. 101-109, 1973.

[2] T. A. Nunn, and J. B. Angell, "An IC absolute pressure transducer with built-in reference chamber," in *Indwelling and Implantable Pressure Transducers*, D. G. Fleming, W. H. Ko, and M. R. Neuman, Eds. Cleveland, OH: CRC Press, 1977.

[3] W. H. Ko, J. Hynecek, and S. F. Boettcher, "Development of a miniature pressure transducer for biomedical applications," *IEEE Trans. Electron Devices*, vol. ED-26, pp. 1896-1905, 1979.

[4] J. M. Borky and K. D. Wise, "Integrated signal conditioning for silicon pressure sensors," *IEEE Trans. Electron Devices*, vol. ED-26, pp. 1906-1910, 1979.

[5] M. Esashi, S. Nomoto, R. Quintero, and T. Matsuo, "Fabrication of biomedical miniature pressure transducer using IC techniques," *Trans. Soc. of Instrument and Control Eng. of Japan*, vol. 15, pp. 959-964, 1979.

[6] C. S. Sander, J. W. Knutti, and J. D. Meindl, "Monolithic capacitance pressure transducer-IC with pulse period output," *IEEE Trans. Electron Devices*, vol. ED-26, pp. 189-192, 1979.

[7] R. L. Meek, "Electrochemically thinned N/N^+ epitaxial silicon method and application," *J. Electrochem. Soc.*, vol. 118, pp. 1240-1246, 1971.